AERODYNAMIC PERFORMANCES OF THE COMBINED CYCLE INLET

Shinji Kubota* Kouichirou Tani, Goro Masuya***
***Tohoku University, **Japan Aerospace Exploration Agency**

Keywords: *combined cycle engine, inlet, aerodynamics, space plane*

Abstract

Ramp compression type inlets for the combined cycle engine were investigated in Mach 4 wind tunnel. Geometries of the inlet models were changed to clarify their effects to the aerodynamic performances and the starting characteristics. A bent cowl improved the starting characteristics by weakening shocks in the inlet duct to suppress the shock induced separation, and by reducing the internal contraction ratio, thus avoiding choking at the inlet throat. With the current geometries, the inlet started with slightly larger internal contraction ratio than that of the Kantrowitz-Donaldson limit. The ratio of the height of the ducted part of the inlet to the incoming boundary layer was found to affect the starting characteristics. The model with higher capture ratio showed the better total pressure recovery performance.

Nomenclature

A = area
h = height
H = height of the side wall
M = Mach number
m_{cap} = mass capture ratio
P = pressure
w = width of the inlet
x = distance from the inlet entrance
α = sidewall sweep back angle
β = cowl lip angle to the free stream
η_{KE} = kinetic energy efficiency
η_{Pt} = total pressure recovery
θ = ramp angle

Subscripts

c = cowl leading edge
in = entrance of the inlet
out = exit of the inlet
t = stagnation condition
w = wall
0 = free stream condition

1 Introduction

One of the promising engines for a space plane is the combined cycle engine which can keep high specific impulse over the wide flight speed range by changing the operating mode [1], such as ”ejector jet mode,” ”ramjet mode,” “scramjet mode” and “rocket mode.” One of the advantages of the combined cycle engine is that it can realize all these operating modes in a single flow passage so that the size and weight of the propulsion system can be reduced.

An inlet is an important part of the combined cycle engine to compress incoming air and to provide it stably to the combustor. Its configuration must be optimized so that it can keep high aerodynamic performances in different operating modes.

There are several geometrical approaches for the combined cycle engine inlets. Ramp compression type is favorable for the combined cycle engine, because its simple geometry allows variable ramp and/or cowl configurations so that the inlets can be adapted to the various operation modes for various speed ranges. It also enables the entrance to be closed during the reentry to the earth atmosphere [2]. More fundamentally, the ramp provides the adequate volume for the rocket engine, which takes a key role in low-speed “ejector jet” mode and “rocket” mode for outer space.

However, in practical designing, variable geometries would be constrained because of

problems such as cooling systems or mechanical complications. To evade the problems, it is preferable to minimize the moving parts and keep the quasi-constant geometries over the wide Mach number range. For that reason, it is important to clarify the effect of the geometries to the performance.

The object of the present study is to investigate the geometrical effect to the aerodynamic characteristics of ramp compression type inlets in the Mach 4 flow condition. Especially, around this Mach number, the inlet starting characteristic is one of the important issues because more efficient "ramjet mode" is required instead of "ejector jet mode" for successful flight-path strategy.

In the current study, the length and the angle of the cowl and the width of the entrance of the inlet were parametrically changed. The flow field was observed by schlieren method and wall pressure measurements. For each configuration, start/unstart conditions were experimentally determined based on the observation, and the effect of the geometrical parameters to the starting characteristic was investigated. The aerodynamic performances such as mass capture ratio and total pressure recovery were also evaluated from the wall and pitot pressure measurements.

2 Experimental Apparatus and Models

The experiments were conducted in the 100 mm × 110 mm blow down Mach 4 wind tunnel in Japan Aerospace Exploration Agency (JAXA), Kakuda. The total pressure and the total temperature of the free stream were 2.2 MPa and the room temperature, respectively. Unit Reynolds number was 1.1×10^8 m^{-1}. The model was mounted at the middle height of the test section.

Figure 1 shows a schematic of the inlet model configuration. The inlet consisted of a cowl, a pair of side walls, a ramp and a top plate which simulated the ventral surface of the vehicle. Overall length of the inlet was 142 mm and the height of the side wall was 16.2 mm. The leading edge of the side wall had a wedge shape with 60 degrees swept back and of 19.3 mm length. Because of this wedge shape, the shock wave was generated and the incoming air was compressed ("side wall compression"). The ramp with 7 degrees compression angle began just at the end of the side wall wedge part, and then the surface of ramp was turned parallel to the free stream direction at the throat.

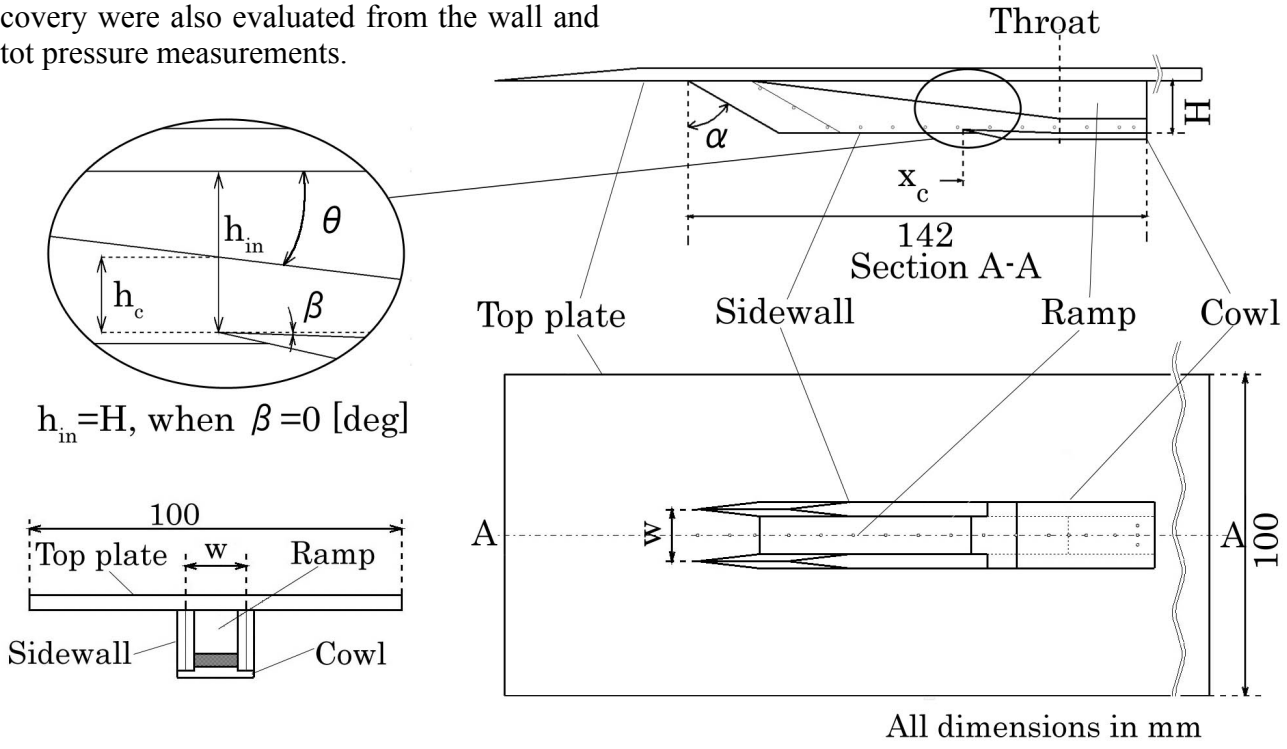

Fig. 1 Schematic of inlet model

The overall contraction ratio ranged from 4 to 5, depending on the geometry. The boundary layer, which developed on the top plate upstream of the model, was ingested into the model. Its thickness at the entrance of the inlet was 1.9 mm, according to the pitot pressure measurements.

The bent cowl was adopted to improve the starting characteristics of the inlet, aiming the reductions of the internal contraction, and weakening the cowl shock wave, which induces a boundary layer separation. The cowl was bent at the position where the ramp surface turns to parallel to the free stream direction, i.e. the throat position.

The less number of engine modules reduces the mass of the sidewalls, and also decreases the friction loss due to the smaller wet surface area. Therefore, the wider form module is expected to show better performances of entire propulsion system. To investigate the influence of the engine cross sectional aspect, the inlet models with three values of the width-to-height ratio w/H = 1, 1.5, 2, were examined. Since the horizontal contraction ratio of side wall geometry changed in accordance with w/H, the height of the throat was adjusted so that the overall contraction ratio of the inlet is fixed to be 5 for non-bending cowl.

Visualization by the schlieren method was adopted and outer flow around the inlet was observed. Pitot pressures at the inlet entrance and at 5 mm upstream of the inlet exit were measured. The wall pressures along the top wall center line, the cowl center line, and the side wall line of 14.1 mm height from the top plate were measured. The performances such as starting characteristics, mass capture ratio, and total pressure recovery ratio of the inlets were evaluated from these measured values. The pressure was measured with the mechanical scanning device (Scanivalve®) with 100 psi (700 kPa) range sensor. The data were then A/D converted and stored to PC. End-to-End uncertainty of the pressure values was within 0.5 %.

3 Results and Discussion

3.1 Wall Pressure Distributions

Figure 2 shows the wall pressure distributions on the top wall of the inlet, for the various cowl angles with fixed cowl leading edge position. The wall pressure, P_w, is normalized by the total pressure of the wind tunnel, Pt_0, and the distance from the entrance, x, is normalized by the height of the side wall, H. The pressure increased at x/H = 1.7 due to the shock wave from the ramp corner. In case of β = 0°, the wall pressure rose again upstream of the cowl lip, and the separation shock was observed with the visualization. In case of β = 2°, the second wall pressure rise occurred downstream of the cowl lip, and no separation shock was observed. With the larger β, the pressure always rose downstream of the cowl lip. The bent cowl showed the effect of relieving the pressure rise and the consequent separation forming.

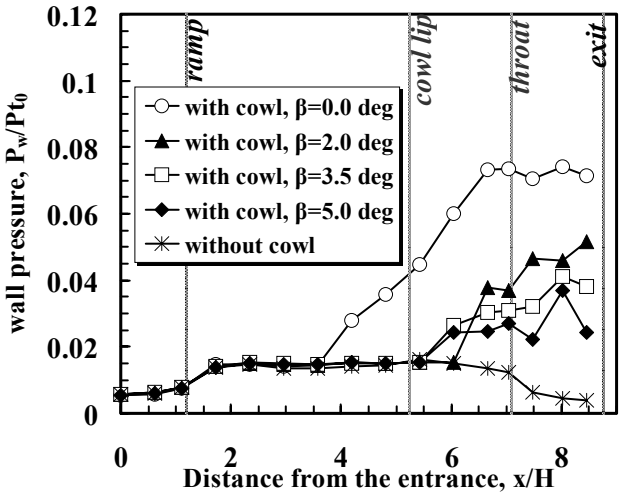

Fig. 2 Effect of bent cowl on wall pressure distributions on the top wall
(w/H=1.0, α=60 deg, θ=7 deg, x_c/H=5.25).

3.2 Starting Characteristics

3.2.1 Categorization of Flow Field

As was depicted, the cowl created high pressure field in its downstream region, where all four sides of the flow passage were surrounded by the solid walls. Inlet "unstart," occurred in the following two manners. One was that the flow was choked by the quasi-one-dimensional constraint. The Kantrowitz-

Donaldson condition [3] (referred as KD, hereafter) corresponds to this sort of constrain. This condition describes the relation between the Mach number at the entrance of the internally converging duct, and the "in-and-out" area ratio of the duct. In this relation, it is assumed that the flow, which decelerates to the subsonic speed by the normal shock wave attached at the entrance of the duct, is choked at the end of the duct. As for the current study, the critical internal contraction ratio A_c/A_{out} was defined according to the KD condition. Here, A_c is the area of the cross section at the cowl leading edge, and A_{out} is the area at the exit of the inlet (see Fig.3).

The other case was that the large separation of the boundary layer which occurred due to the large adverse pressure gradient caused by the internal flow structure. One parameter which influences the magnitude of the adverse pressure gradient is an internal contraction angle of the inlet, defined as θ-β (Fig.3). With the lager internal contraction angle, shockwaves formed in the duct became stronger and it caused the separation of the boundary layer on the ramp surface. This separation led to form the separation shock wave upstream of the cowl lip that made the additional spillage of the incoming air.

Here, the flow conditions in the inlet were categorized in three statuses.

(A) The separation shock wave was not formed upstream of the cowl leading edge. (start)

(B) The separation shock wave was formed upstream of the cowl leading edge. However, the flow was not choked upstream of the throat of inlet. (unstart, non-choked)

(C) The separation shock wave was formed upstream of the cowl leading edge. Concurrently, the flow was choked around the throat of inlet. (unstart, choked)

Figure 4 shows typical wall pressure distributions of an example of these 3 flow statuses. The existence of the separation shock wave was detected from these wall pressure distributions and the visualization by the schlieren method. No significant difference could be observed in the top wall pressure distribution of (B) and (C). Only the throat conditions could determine their distinctiveness. In the current study, choking was determined so that the mass flow at the exit calculated from the pitot pressure reached to more than 95 % of the choked mass flow which was estimated from the total temperature, the total pressure and the cross section area at the model exit.

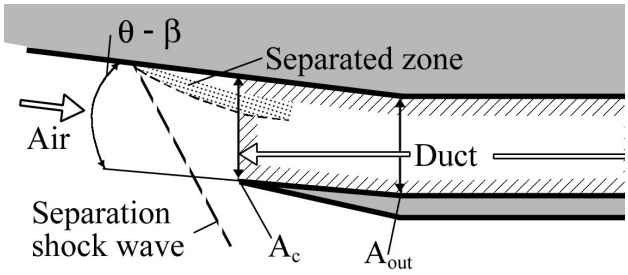

Fig. 3 Definition of inlet geometries and separation shock wave

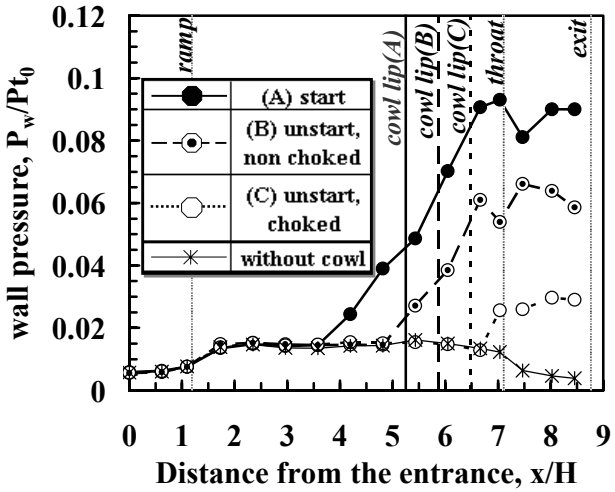

Fig. 4 Example of 3 flow statuses: wall pressure distributions on the top wall (w/H=1.0, α=60°, θ=7°, β=0°).

Figure 5 shows the relation between the geometry of the inlet and the starting limits. The horizontal-axis refers to the internal contraction ratio, A_c/A_{out}, and the vertical-axis refers to the internal contraction angle, θ- β. Note that in case that the data take the same coordinate, the marks plotted in the figure were slightly shifted along the vertical direction. There were four kinds of θ- β, i.e. 2°, 3.5°, 5°, and 7°. The three

flow conditions (A), (B), (C) are shown with a solid symbol (start), a dotted symbol (unstart, non choked), and an open symbol (unstart, choked). The region of Fig. 5 can be roughly divided into the three flow conditions.

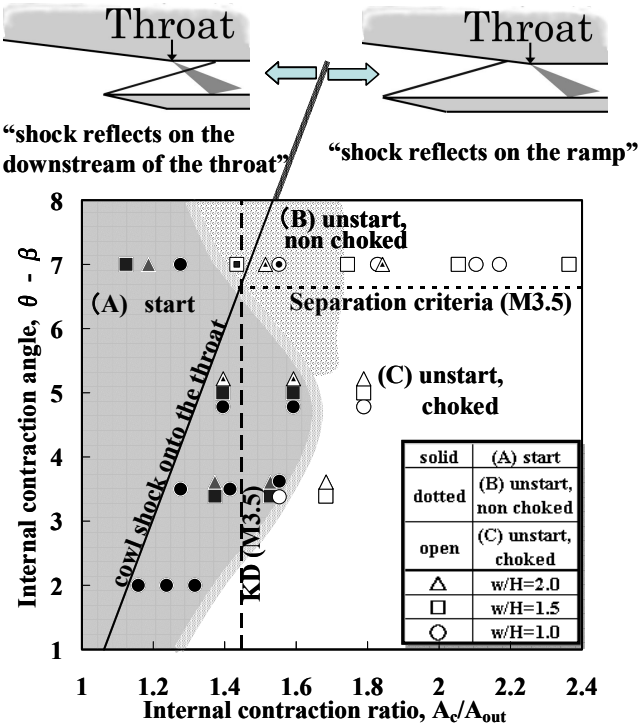

Fig. 5 Starting characteristics and inlet geometry

3.2.2 Effect of Internal Contraction Ratio

In Fig. 5, the KD condition for the Mach 3.5, i.e. A_c/A_{out} = 1.45, is shown with a dashed line, since the free stream of Mach 4.0 decelerated to that speed by the ramp shock wave of 7° deflection angle. Be noted that the "effective" KD condition limit becomes somewhat less than 1.45, due to the displacement by the boundary layer. Most of the inlets with the internal contraction ratio below KD conditions started.

Van Wie et al. conducted an inlet experiment to investigate the major factor of the starting characteristics [4]. In case the ratio of boundary layer to the height of the inlet was sufficiently small, they concluded that the starting contraction ratio could be predicted by the KD conditions, roughly within 10 % accuracy. In the present study, the boundary of the starting limit was also located within 10 % of the KD conditions.

3.2.3 Effect of Internal Contraction Angle

The solid line in Fig. 5 indicates the condition at which the cowl shock wave impinges to the throat. On the right side of the line the cowl shock wave reflects on the ramp, and on the left side, it does on the downstream of the throat. In case with $\theta-\beta$ = 7°, no inlets on the right side of the line started, while some on the left side of the line started. In the latter cases, the expansion wave from the throat corner suppressed the propagation of the boundary layer separation to the ramp surface, which was initially prompted by the cowl shock wave. On the other hand, some of the inlets started when $\theta-\beta$ was less than 5°, even when the cowl shock wave impinged on the ramp surface. The pressure rise on the ramp surface by the cowl shock wave becomes larger with the larger contraction angle, and with a certain pressure rise, the boundary layer separation is inevitable. There proposed several boundary layer separation models. Mager [5] has postulated a model of the shock-induced separation and formulated the relation between the Mach number and the critical pressure rise required for the boundary layer separation. This separation criterion was applied for the pressure rise on the ramp surface, and is also shown in Fig. 5 with a dotted line. Though for an actual unstart, the separation front has to go as further upstream as to the duct entrance, the criterion gives the "safer" limit for starting.

3.2.4 Effect of Cross Sectional Aspect

In Fig. 5, the parameter of w/H is symbolized with a circle (w/H = 1.0), a square (w/H = 1.5), and a triangle (w/H = 2.0). There are no significant difference with the difference of w/H, except the case that $\theta-\beta$ = 5°and A_c/A_{out} = 1.4 ~ 1.6. In this case, the inlets with w/H = 1 and 1.5 started, but the inlet with w/H = 2.0 did not. The test with thinner incoming boundary layer was conducted by removing the part of top

plate upstream of the inlet (foreplate), and the inlet with w/H = 2.0 turned to start (Figure 6). In the current sort of configuration, as the w/H becomes lager, the height of the throat becomes smaller. The result suggested that the ratio of the duct height to the thickness of the boundary layer was one of the factors for the starting characteristics.

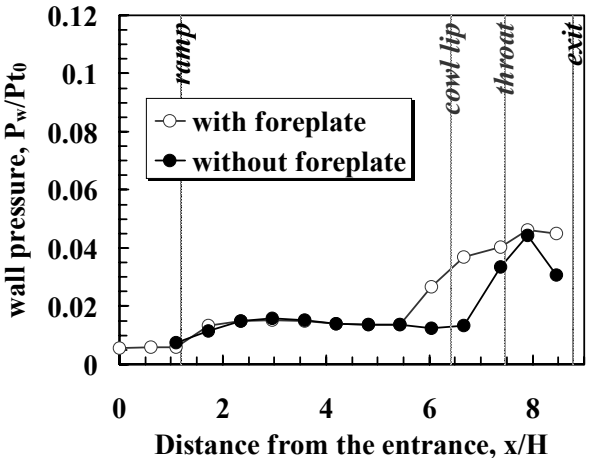

Fig. 6 Influence of thickness of boundary layer on wall pressure distributions on the top wall (w/H=2.0, α=60 deg, β=2°, θ=7 °, x_c/H=6.41)

3.3 Inlet Aerodynamic Performances

3.3.1 Geometrical Effects

Figure 7 shows the mass capture ratio for all tested configuration. The mass capture ratio, $m_{cap,}$ is plotted as a function of A_c/A_{in}, where A_{in} is the area of the cross section at the inlet entrance. The same symbols as those in Fig. 4 are employed.

By assuming two-dimensional oblique shock wave emanated from the ramp corner, the streamline which attaches to the cowl lip could be estimated, and the mass capture ratio could be defined as the ratio of the height of this streamline at the entrance to the overall inlet height. The result of this calculation is also shown in Fig. 7, with a solid line.

The captured mass flow rate m_{cap} changed linearly to A_c/A_{in} as long as the inlet starts. Although it gave a little greater value, the calculation had well estimated the gradient factor of m_{cap} to A_c/A_{in}. The comparison indicated that the most of the spillage was created by the ramp shock.

When the inlet was in the unstart condition without choking, m_{cap} took a greater value with increment of A_c/A_{in}. In the current definition, the increment of A_c/A_{in} corresponded to two situations. One was that β became smaller and the other case was that the cowl lip located further upstream. Although there was the separation shock which produced the additional spillage, the tendency revealed that the amount of the flow scooped by the longer cowl increased to some extent.

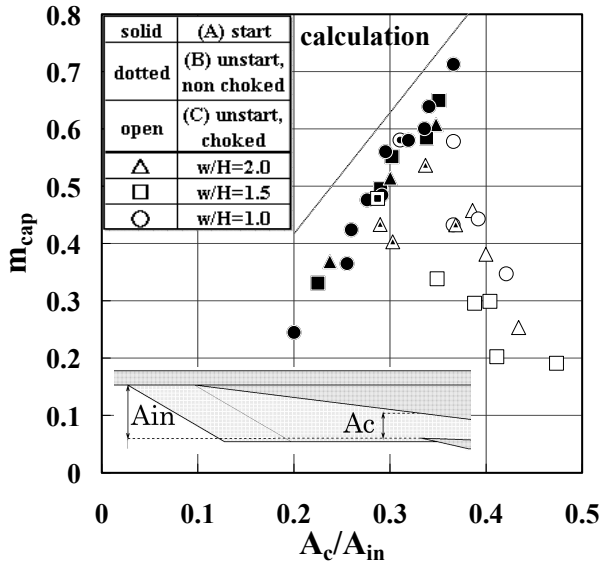

Fig. 7 Mass capture ratio and inlet geometry

In case of the unstart with choking, as A_c/A_{in} was increased, m_{cap} decreased. In this case, the separation shock wave shifted further upstream, and drastically increased the spillage of the main stream which had high total pressure, and thus it resulted in decreasing the total pressure of the incoming flow. In the choked flow field, less total pressure leads to decrease of m_{cap} for the constant area and total temperature.

Figure 8 shows the total pressure recovery, $\eta_{Pt,}$ for all tested configuration. η_{Pt} is a ratio between the mass averaged total pressure at the entrance and the exit of the inlet. Here, η_{Pt} is plotted as a function of m_{cap}. In the started condition, η_{Pt} increased as the m_{cap} increased.

When m_{cap} increased, in general, the compression ratio becomes larger, and thus the total pressure loss by the shock waves became larger. On the other hand, the increase of m_{cap} also led to decrease the ratio of mass flow of the boundary layer to that of the main stream, and thus to increase the mass averaged total pressure. The result indicated the latter effect was more dominant in the current geometry. In the choked condition, η_{Pt} increased linearly to m_{cap}. The reason is that the choked mass flow is proportional to the total pressure with the constant total temperature and the constant area. In case of the unstart with non-choking, η_{Pt} distributed between the values of the start and the unstart with choking, and it also tend to increased as m_{cap} increased.

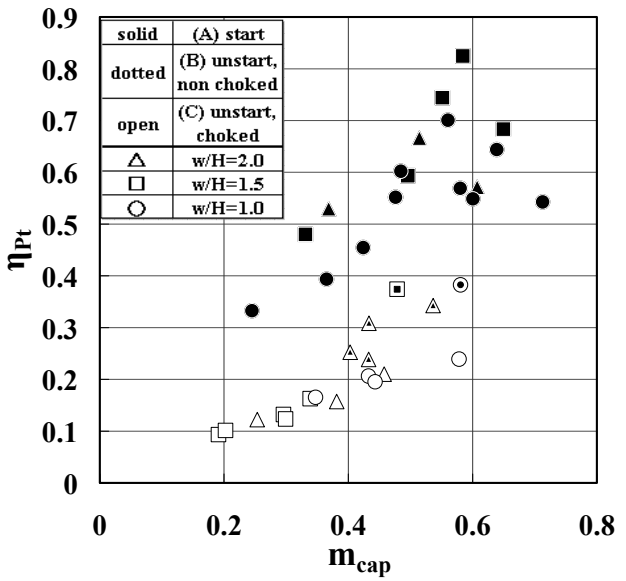

Fig. 8 Relation between total pressure recovery and mass capture ratio

3.3.2 Comparison with the Side Wall Compression Type Inlets

Tani et al. [6, 7] tested the side wall compression type inlet with almost same scaled models as the present study to examine the geometrical effects to the starting characteristics. Figure 9 shows the comparison of the kinetic energy efficiency, η_{KE}, between the ramp compression inlet and the side wall compression inlet. η_{KE} is plotted as a function of the exit to free stream Mach number ratio, M_{out}/M_0. The result of the ramp compression inlet and the side wall compression inlet are plotted with the solid symbol and the open symbol, respectively. Since the trichotomous classification introduced earlier section cannot be applied to the status of flow field in the side wall compression inlet, here dichotomous categorization (start / unstart) is adopted, based on the existence of the separation shock upstream of the cowl lip. The conditions are shown with the symbol of a circle (start) and a triangle (not start). Note that the values were normalized by the free stream quantities instead of the averaged one at the inlet entrance. The empirical estimations by Waltrup [8] and Tani [7] are also shown with solid and dashed lines, respectively.

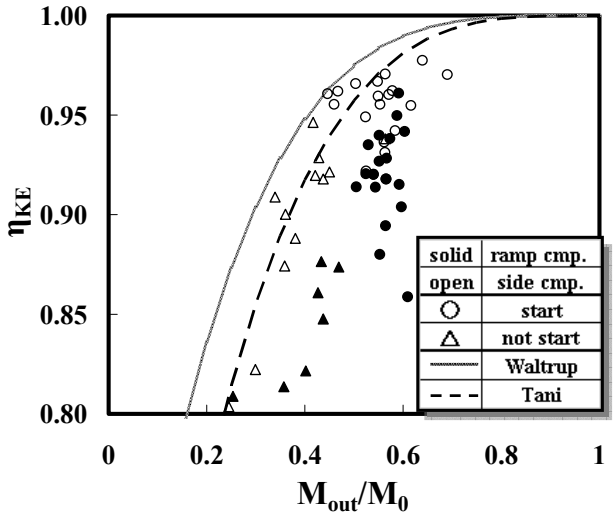

Fig. 9 Comparison of efficiencies between ramp compression inlet and sidewall compression inlet

In general, the side wall compression inlet showed better performance than the ramp compression inlet. One of the reasons for the lower performance of the ramp inlet was the difference of the point where pitot pressures were measured. For the side wall compression inlet, the data were obtained at the end of convergent section, while they were captured at the exit of the model for the ramp inlet. Thus, the values of the ramp inlet were affected by the shock waves in the ducted part.

4 Conclusions

The ramp compression type inlets for the combined cycle engine were experimentally investigated in Mach 4 flow condition. The model geometries were changed parametrically, and the following points were clarified.

(1) The flow field in the ramp type inlet was categorized into three conditions, i.e. start / unstart without choking / unstart with choking.
(2) The bent cowl improved the starting limit of the inlet.
(3) The maximum internal contraction ratios with which the inlets started were around the Kantrowitz - Donaldson limits.
(4) The smaller ratio of the height of the duct section to the thickness of the incoming boundary layer led the unstart of the inlet
(5) The loss of the total pressure by spilling the main stream which has high total pressure was greater than that by the shock wave formed in the inlet, thus the total pressure recovery became higher with the higher capture ratio.
(6) The smaller internal contraction angle improved the starting characteristic. The shock impinging point on the ramp surface was found to be one of the elements for the starting characteristic.

Acknowledgement

The authors acknowledge Takeshi Kanda of JAXA for useful advices and Kenji Kudo and Kanenori Kato of JAXA for their tremendous help in conducting the experiments.

References

[1] Russell, D. and Corin, S., "Combined Rocket and Airbreathing Propulsion Systems for Space-Launch Applications," *Journal of Propulsion and Power*, Vol. 14, No. 5, 1998, pp. 605-612.

[2] Kanda, T. and Kudo, K., "Cooling Requirement of the Combined Cycle Engine in Descending Flight," ISTS Paper 2004-a-12, 2004.

[3] .Crocco, L., "One-Dimensional Treatment of Steady Gas Dynamics," *Fundamentals of Gas Dynamics*, edited by H. W. Emmons, 2nd ed., Princeton University Press. Princeton, 1967, pp. 184-190.

[4] Van Wie, D. M., Kwok, F. T. and Walsh, R. F., "Starting Characteristics of Supersonic Inlet," AIAA Paper 96-2914, 1996

[5] Mager, A., "On the Model of the Free, Shock-Separated, Turbulent Boundary Layer," Journal of the Aeronautical Sciences, Vol. 23, Feb. 1956, pp. 182-184

[6] Tani, K. Kanda, T. and Tokunaga, T., "Starting Characteristics of Scramjet Inlets," *Proceedings of 11th ISABE*,. Tokyo, 1993, pp. 1071-1080

[7] Tani, K., Kanda, T., Kudo, K., Murakami, A., Komuro, T., and Itoh, K., "Aerodynamics Performance of Scramjet Inlet Models with a Single Strut, " AIAA Paper 93-0741, Jan. 1993.

[8] Waltrup, P.J., Billig, F.S., and Stockbridge, D., "Engine Sizing and Integration Requirements for Hypersonic Airbreathing Missile Applications," *AGARD CP-307*, 1982.